Molecular Biology of the Cell
Vol. 17, 3664–3677, August 2006

Regulated Synthesis and Functions of Laminin 5 in Polarized Madin-Darby Canine Kidney Epithelial Cells

Grace Z. Mak,* Gina M. Kavanaugh,* Mary M. Buschmann,* Shaun M. Stickley,* Manuel Koch,† Kathleen Heppner Goss,* Holly Waechter,* Anna Zuk,‡ and Karl S. Matlin*

*Laboratory of Epithelial Pathobiology, Department of Surgery, University of Cincinnati, Cincinnati, OH 45267-0581; †Center for Biochemistry, Center for Molecular Medicine, and Department of Dermatology, University of Cologne, Cologne 50923, Germany; and ‡Genzyme Corporation, Framingham, MA 01701

Submitted November 22, 2005; Revised May 31, 2006; Accepted June 1, 2006
Monitoring Editor: Asma Nusrat

Renal tubular epithelial cells synthesize laminin (LN)5 during regeneration of the epithelium after ischemic injury. LN5 is a truncated laminin isoform of particular importance in the epidermis, but it is also constitutively expressed in a number of other epithelia. To investigate the role of LN5 in morphogenesis of a simple renal epithelium, we examined the synthesis and function of LN5 in the spreading, proliferation, wound-edge migration, and apical–basal polarization of Madin-Darby canine kidney (MDCK) cells. MDCK cells synthesize LN5 only when subconfluent, and they degrade the existing LN5 matrix when confluent. Through the use of small-interfering RNA to knockdown the LN5 α3 subunit, we were able to demonstrate that LN5 is necessary for cell proliferation and efficient wound-edge migration, but not apical–basal polarization. Surprisingly, suppression of LN5 production caused cells to spread much more extensively than normal on uncoated surfaces, and exogenous keratinocyte LN5 was unable to rescue this phenotype. MDCK cells also synthesized laminin α5, a component of LN10, that independent studies suggest may form an assembled basal lamina important for polarization. Overall, our findings indicate that LN5 is likely to play an important role in regulating cell spreading, migration, and proliferation during reconstitution of a continuous epithelium.

INTRODUCTION

Epithelia line the surfaces of multicellular organisms, acting as semipermeable barriers between the internal milieu and the outside world. To carry out this function, epithelial cells are structurally and functionally polarized (Nelson, 2003). Epithelial cell polarity arises during embryonic development and regenerates after injury (Fish and Molitoris, 1994; Zuk *et al*., 1998; Nelson, 2003). Although the details are still not clear, it seems many of the factors responsible for signaling polarization of epithelial cells are shared with other types of cells that respond asymmetrically to particular stimuli (Nelson, 2003). What sets epithelial cells apart, however, is that they are capable of forming a continuous sheet of polarized cells, each with exactly the same orientation relative to each other and the extracellular environment.

There is abundant evidence that the environmental signals or "spatial cues" for coordinated polarization of epithelial cells are adhesive interactions, both between cells and with the extracellular matrix (Nelson, 2003). When suspended individually, epithelial cells are depolarized; cell–cell or cell–matrix interactions alone induce at least a degree of polarity, whereas both classes of adhesion are required for full polarization (Vega-Salas *et al*., 1987). Cell–cell adhesion is facilitated primarily by E-cadherin and its associated proteins, and signals from these molecules are required for polarization (Vega-Salas *et al*., 1987; Nelson, 2003). In contrast, the exact identities and particular functions of both extracellular matrix receptors and ligands responsible for signaling polarization from the substratum are unknown.

In tissues, epithelial cells reside on a basal lamina composed primarily of isoforms of laminin (LN), collagen type IV, and heparan sulfate proteoglycans (Yurchenco, 1994; Li *et al*., 2005). Of these molecules, there is evidence that laminins are critically involved in polarization (Klein *et al*., 1988; Sorokin *et al*., 1990; Zinkl *et al*., 1996; Ekblom *et al*., 1999; Li *et al*., 2003; Miner and Yurchenco, 2004). In particular, laminin has been implicated in the polarization of both the developing kidney tubular epithelium and the Madin-Darby canine kidney (MDCK) cell line through the use of function-blocking antibodies (Klein *et al*., 1988; Sorokin *et al*., 1990; Zinkl *et al*., 1996). Furthermore, deletion of the γ1 subunit of laminin in mouse embryonic stem cells blocks epiblast polarization in vitro, whereas mutations in genes for both laminin subunits and laminin receptors lead to disrupted epithelial polarity in *Caenorhabditis elegans* and *Drosophila* (Li *et al*., 2003; Miner and Yurchenco, 2004).

Laminins are a family of large heterotrimeric glycoproteins consisting of at least 15 members composed of combinations of five α, three β, and three γ subunits (Colognato and Yurchenco, 2000; Miner and Yurchenco, 2004). The prototypical laminin structure is cruciform, with three arms contributed by fibrous and globular domains, and a rigid stalk made up of a coiled-coil of all three subunits. The terminal regions of each arm are capable of associating with similar domains on other molecules to form a polymer network, whereas the end of the stalk interacts with a variety of cellular receptors (Miner and Yurchenco, 2004). Assembly of

This article was published online ahead of print in *MBC in Press* (http://www.molbiolcell.org/cgi/doi/10.1091/mbc.E05–11–1070) on June 14, 2006.

Address correspondence to: Karl S. Matlin (karl.matlin@uc.edu).

laminin into a basal lamina is believed to be initiated by monomer association with the cell surface, followed by polymerization dependent on laminin concentration and divalent cations (Yurchenco, 1994; Cheng *et al*., 1997; Colognato *et al*., 1999; Odenthal *et al*., 2004; Li *et al*., 2005). Some laminin isoforms diverge from this model by possessing one or more truncated subunits that render them less able to polymerize (Cheng *et al*., 1997; Miner and Yurchenco, 2004; Odenthal *et al*., 2004).

Our laboratory has been studying the involvement of laminin in the polar morphogenesis of epithelia both in vitro using MDCK cells and during regeneration of the renal epithelium after ischemic injury in vivo. In the rat kidney, we found that LN5, a truncated isoform moderately expressed only in the renal papilla under normal conditions, is expressed at high levels in many regions of the kidney during regeneration (Carter *et al*., 1991; Rousselle *et al*., 1991; Miyazaki *et al*., 1993; Miner, 1999; Zuk and Matlin, 2002). Based upon these results, we hypothesized that LN5 might be important in facilitating the reconstitution of an intact, polarized epithelium after injury.

In this article, we report that LN5 is transiently synthesized by MDCK cells during regeneration of a confluent epithelium and is required to both stimulate proliferation and regulate cell spreading. It is not, however, necessary for apical–basal polarization per se, at least in two-dimensional, monolayer culture. These findings indicate that LN5 may have a widespread role in facilitating epithelial regeneration in more instances than previously recognized.

MATERIALS AND METHODS

Cell Culture

Stock cultures of MDCK cells (strain II, Heidelberg isolate, passages 7–35) were grown in DMEM (high glucose) supplemented with 5% fetal bovine serum (FBS) and 10 mM HEPES-KOH, pH 7.3, at 37°C in an atmosphere of 5% CO_2 as described previously (Matlin *et al*., 1981).

In polarization experiments, cells were grown on uncoated Transwell permeable supports (2.4 cm in diameter, pore size, 0.4 μm; Corning-Costar, Acton, MA). After prewetting the supports with medium, 1.5 ml of complete growth medium containing 1.5×10^6 cells was added to the upper chamber, and 2.5 ml of medium was added to the bottom. Under these conditions, a confluent and polarized monolayer formed after 18–24 h incubation, as determined by immunofluorescence of apical and basolateral markers and measurements of transmonolayer resistance (Zinkl *et al*., 1996).

Antibodies

Laminin Isoforms. Antibody 8LN5 (affinity-purified rabbit polyclonal anti-kalinin; 0.43 mg/ml) was obtained from Dr. Robert Burgeson (Massachusetts General Hospital, Boston, MA), and was used for immunofluorescence, immunoprecipitation, and immunoblotting. This antibody reacts with all three subunits of human LN5 by immunoblotting and specifically stains the basement membrane underlying human epidermis (Zuk and Matlin, 2002). Mouse monoclonal anti-kalinin B1 (0.25 mg/ml), directed against the β3 laminin subunit, was purchased from BD Biosciences Transduction Laboratories (Lexington, KY) (catalog no. 610424) and used for immunoblotting; it was not suitable for immunofluorescence or immunoprecipitation. Affinity-purified rabbit anti-LN1 (0.6 mg/ml) was purchased from Sigma-Aldrich (St. Louis, MO) (catalog no. L9393) and used for immunofluorescence and immunoprecipitation.

Integrins. Antibody AIIB2 (monoclonal rat anti-mouse β1 integrin) was used for adhesion assays as a culture supernatant prepared from hybridomas obtained from the Developmental Studies Hybridoma Bank (Department of Biological Sciences, The University of Iowa, Iowa City, IA) (Hall *et al*., 1990). Antibody GoH3 (monoclonal rat anti-human α6 integrin; 1 mg/ml) was purchased from BD Biosciences PharMingen (San Diego, CA) (catalog no. 555734); and was used for adhesion assays and immunoprecipitation (Sonnenberg *et al*., 1987). Rabbit polyclonal anti-β1 integrin was prepared against a synthetic peptide corresponding to the carboxy-terminal 37 amino acids of human β1 integrin and was used for immunoblotting.

Other Primary Antibodies. Culture supernatants containing mouse monoclonal antibodies (mAbs) against the apical MDCK protein gp135 (Ojakian and Schwimmer, 1988; Meder *et al*., 2005) and the basolateral marker E-cadherin were prepared from the 3F21D8 hybridoma (a kind gift of George Ojakian, SUNY Downstate, Brooklyn, NY) and the rr1 hybridoma (a kind gift of Barry Gumbiner, University of Virginia School of Medicine, Charlottesville, VA) (Gumbiner and Simons, 1986), respectively. The supernatants were used without dilution to stain MDCK cells grown on Transwell supports. Staining of cells labeled with bromodeoxyuridine was accomplished with rat monoclonal anti-bromodeoxyuridine (BrdU) (catalog no. ab6326-250, 1 mg/ml; Abcam, Cambridge, MA).

Secondary Antibodies. For immunofluorescence, affinity-purified goat anti-mouse, -rabbit, and -rat secondary antibodies conjugated to Alexa Fluor-488 or -555 were purchased from Molecular Probes-Invitrogen (Carlsbad, CA) (2 mg/ml). For immunoblotting, affinity-purified polyclonal donkey anti-rabbit or anti-mouse IgG (heavy and light chains) conjugated to peroxidase (0.4 mg/ml) were purchased from Jackson ImmunoResearch Laboratories (West Grove, PA). When available, all secondary antibodies were highly cross-adsorbed against other species.

Other Reagents

Collagen (type I from rat tail tendon, 4 mg/ml) for coating culture surfaces was purchased from Upstate Biotechnology (Lake Placid, NY) (catalog no. 08-115). LN5 was purified from human keratinocyte conditioned culture medium by affinity chromatography using the 6F12 mAb against the laminin β3 chain as described previously (Eble *et al*., 1998). The preparation was pure and intact as judged by SDS-gel electrophoresis (our unpublished data) and supported the adhesion of epidermal carcinoma cells. Phalloidin conjugated to Alexa Fluor-488 was purchased from Molecular Probes-Invitrogen and used for fluorescence microscopy by diluting a methanol stock (200 U/ml) 1:80. All other chemicals were reagent grade.

SDS-Gel Electrophoresis and Immunoblotting

SDS-PAGE was conducted in a minigel apparatus (Bio-Rad, Hercules, CA) using Laemmli buffers (Laemmli, 1970). For immunoblotting, cell cultures were extracted directly with SDS extraction buffer (50 mM Tris-HCl, pH 8.8, 2% SDS, and 5 mM EDTA) supplemented with Complete protease inhibitors (Roche Diagnostics, Indianapolis, IN). The extract was then sheared by multiple passes through a 22-gauge syringe needle, immediately heated for 3 min at 95°C, mixed in a 1:3 ratio with 40% sucrose, 5 mM dithiothreitol (DTT), and 0.08% bromphenol blue, and reheated for 3 min at 95°C. Samples were then alkylated at 37°C for 15 min with 4 mM iodoacetamide before loading on the SDS gel. MDCK cell endogenous extracellular matrix was prepared by removing the cell layer with Triton X-100 and NH_4OH as described previously (Le Beyec *et al*., 1997) and then extracting the matrix proteins directly with SDS extraction buffer.

Immunoblotting was carried out with a Bio-Rad semidry apparatus exactly as described previously (Zuk and Matlin, 2002). Primary antibodies were incubated with membranes sealed in plastic bags overnight at 4°C followed, after washing, by a 1-h incubation with a horseradish peroxidase-conjugated secondary antibody diluted at 1:5000. Bands were visualized by reacting membranes with enhanced chemiluminescence reagents (GE Healthcare, Little Chalfont, Buckinghamshire, United Kingdom) and exposing them to x-ray film. Primary antibody dilutions were 1:1500 for polyclonal anti-LN5 and 1:1000 for polyclonal anti-β1 integrin.

Metabolic Labeling and Immunoprecipitation

Short-term (4-h) metabolic labeling of MDCK cells was accomplished by incubating 35-mm-diameter cultures in serum-free DMEM (high glucose)/10 mM HEPES, pH 7.3, lacking methionine and cysteine (labeling medium) for ~15 min at 37°C, 5% CO_2 to deplete amino acid pools, and labeling with 100 μCi of [^{35}S]Met)/Cys for 4 h. Long-term (18–24 h) labeling was conducted (without washing or preincubation) in DMEM/10 mM HEPES, pH 7.3/5% FBS containing 1/10 the normal amount of unlabeled methionine and cysteine and 100 μCi [^{35}S]Met/Cys at 37°C, 5% CO_2. After completion of labeling, the medium was removed and the cultures were washed twice with ice-cold phosphate-buffered saline (PBS) before extraction.

For immunoprecipitation, cells were extracted on ice with radioimmunoprecipitation assay (RIPA) buffer (10 mM Tris-HCl, pH 7.5, 0.5% SDS, 1.0% Igepal-CA630, 0.15 M NaCl, and 1.0% sodium deoxycholate) supplemented with Complete protease inhibitors. The extracts were filtered through Ultrafree-CL centrifugal filters (Millipore, Billerica, MA) and then incubated with antibodies overnight at 4°C. LN5 and presumptive LN10 were immunoprecipitated with 1:200 dilutions of antibody 8LN5 and anti-LN1, respectively. Integrin α6 was immunoprecipitated with 1:250 dilution of GoH3 antibody. Immune complexes were captured with 30 μl of washed protein A-Trisacryl or protein G-agarose beads (Pierce Chemical, Rockford, IL). Immunoprecipitated proteins were solubilized and reduced by heating for 3 min at 95°C in SDS-gel sample buffer (0.16 M Tris-HCl, pH 8.8, 4 mM EDTA, 16% sucrose, 0.16% bromphenol blue, 20 mM DTT, and 2% SDS) and then alkylated before loading on an SDS-gel. To visualize radioactive bands, gels were infiltrated

with Enhance (PerkinElmer Life and Analytical Sciences, Boston, MA), dried, and exposed to x-ray film.

In some cases, LN5 was immunoprecipitated not only from extracts of long-term labeled cells but also from the culture medium. To accomplish this, culture medium was collected, centrifuged to remove any particulate matter, and antibodies were added directly to the supernatant.

Immunofluorescence and Confocal Microscopy

Indirect immunofluorescence staining of MDCK cells grown on glass coverslips was conducted on formaldehyde-fixed cells as described previously (Prahalad *et al*., 2004). LN5 was detected by staining with 10 μg/ml 8LN5; presumptive LN10 was detected with a 1:100 dilution of anti-LN1. Alexa Fluor-conjugated secondary antibodies were diluted 1:500. Stained coverslips were viewed on a Zeiss Axioskop fluorescence microscope with a 63×, 1.4 numerical aperture (NA) PlanApo or 40×, 1.3 NA PlanNeofluor oil immersion objective and Nomarski optics, and photographed with an Axiocam MRm digital camera using Axiovision software (Carl Zeiss, Thornwood, NY).

MDCK cells grown in Transwell chambers were fixed for 30 min at room temperature with 3% formaldehyde in PBS at room temperature and quenched for 15 min with freshly prepared 0.1% $NaBH_4$/PBS at room temperature with gentle agitation. Cells were permeabilized by incubation with 0.1% Triton X-100 in PBS for 4 min. At this point, the filters were cut from their plastic support with a scalpel blade, transferred cell side up to individual 35-mm plastic Petri dishes, blocked for 30 min at room temperature with 10% goat serum in PBS, and cut into quarters for staining.

Antibody staining was conducted in a moist chamber at room temperature by placing filter quarters cell side up over 100-μl droplets of antibody solutions on sheets of Parafilm and then gently covering the cell side with an additional 100 μl of antibody. The filters were then incubated with the antibody for 30 min at room temperature and washed four times with PBS for 5 min each with agitation in individual 35-mm dishes. Staining with secondary antibodies was conducted identically. When filamentous actin was labeled, dilute fluorescent phalloidin was included with the secondary antibody.

After antibody staining, filter quarters were washed with PBS and 0.1% Triton X-100/PBS and postfixed with 3% formaldehyde/PBS. They were then mounted on glass slides in hard-set Vectashield Antifade mounting solution (Vector Laboratories, Burlingame, CA) under a 22-mm square coverslip supported by four hardened nail polish "feet," and edges sealed with additional nail polish.

Stained filter quarters were imaged with a Zeiss LSM-510 confocal laser scanning microscope in either the XY plane or as a Z-line orthogonal image using a 63×, 1.4 NA PlanApo oil immersion objective. For XY images, the optical slice was ~1.0 μm with a frame size of 1024 × 1024 pixels. For Z-lines, the frame size was 2048 × 2048 pixels with a step size of 0.48 μm. For each experiment, images were collected at identical dynamic range settings. Conventional and confocal digital images were optimized with Adobe Photoshop (Adobe Systems, Mountain View, CA) using linear adjustments of levels, contrast, and brightness.

Adhesion Assay

Adhesion assays in 96-well microtiter plates with and without function-blocking anti-integrin antibodies were conducted essentially as described previously (Schoenenberger *et al*., 1994).

Polymerase Chain Reaction

Laminin α3 and α5 transcripts were detected by combined reverse transcriptase (RT)-PCR. Total MDCK cell RNA was prepared with an RNAeasy kit (QIAGEN, Valencia, CA). RT-PCR was conducted with 1.0 μg of RNA/50-μl reaction with a 10-min annealing step at 25°C, a 12-min reverse transcriptase reaction at 42°C, and 30–40 PCR cycles. Laminin primers were based on the sequences of human transcripts. Laminin α3 primers were 5′-ACAGATGGAGAGGGAAACAAC-3′ (forward) and 5′-ATTTGCCTGCTTGGC TTGG-3′ (reverse), corresponding to nucleotides 1000–1299 of the human sequence. Laminin α5 primers were 5′-GCGACAACTGCCTCCTCTAC-3′ (forward) and 5′-CCAGGTGGTCCTGGGTATC-3′, corresponding to nucleotides 3189–3154 of the human sequence. Canine β-actin primers were 5′-CAAAGCCAACCGTGAGAAG-3′ (forward) and 5′-CAGAGTCCATGACAATACCAG-3′ (reverse), corresponding to residues nucleotides 772-1028 in the canine sequence.

Suppression of Laminin α3 Synthesis with Small-Interfering RNA (siRNA)

A partial canine laminin α3 sequence was determined by automated DNA sequencing at the University of Cincinnati College of Medicine core facility-(Cincinnati, OH) using a PCR product obtained with human specific primers (see PCR protocol). Possible siRNA targets were identified in the PCR product sequence using a computerized algorithm at the Ambion (Austin, TX) Web site (Elbashir *et al*., 2001, 2002). One such sequence that mapped specifically to the laminin α3 transcript was chosen. The sequence (5′-AAATGACTACGAAGCCAAACT-3′) is located at nucleotide 1257 of the canine laminin α3 transcript and nucleotide 1224 of the human laminin α3 transcript (Ensembl Genome Browser; www.ensembl.org).

The efficacy of the target sequence was first tested by transient transfection of RNA duplexes into MDCK cells. Synthetic RNA molecules corresponding to the target sequence and its complement, and control RNAs not corresponding to any known gene, were purchased from Ambion. These were annealed according to recommendations from Ambion and transfected into MDCK cells as siPORT (Ambion) complexes in serum-free DMEM. After 48-h incubation, RNA was prepared from the transfected and mock-transfected cells, and the RNA analyzed by RT-PCR. Based on this, the selected target was determined to knock down laminin α3 mRNA (Figure 5A).

Adenoviral vectors capable of expressing the siRNA targeted to laminin α3 were engineered using the pSIREN-Shuttle vector and Adeno-X-expression vector (Clontech, Mountain View, CA). cDNA oligonucleotides containing the sense and antisense sequences of the siRNA on the same strand separated by a hairpin sequence and flanked by terminator, 3′-EcoRI, and 5′-BamHI restriction sites were purchased from Integrated DNA Technology (Coralville, IA). These were annealed and ligated into the BamHI and EcoRI sites in the pSIREN vector. The hairpin construct and RNA polymerase promoter sequences were then cut from the vector with I-CeuI and PI-SceI and ligated into equivalent sites in Adeno-X DNA. The completed construct was verified by DNA sequencing.

Adenovirus was produced by transfection of the Adeno-X-hairpin construct into human embryonic kidney (HEK)-293 cells according to the manufacturer's directions (Clontech). The primary viral stock was titered with an Adeno-X Rapid Titer kit (Clontech) and was used to grow subsequent viral stocks. Adenoviral vector stocks capable of laminin α3 knockdown were called "Ad-D5." A stock of adenovirus expressing Lac-Z (Ad-LacZ) was prepared in HEK-293 cells from original virus provided by Andrew Lowy (University of Cincinnati, Department of Surgery); this was used in experiments as a control for adenovirus infection.

In some cases, adenovirus was purified by centrifugation in OptiPrep (iodixanol; Axis-Shield USA, Norton, MA) step gradients of 15–25–40–54% centrifuged overnight at 100,000 × *g* and 4°C. The viral band was harvested between the 25 and 40% layers and used directly without dialysis. Typical stock virus titers were 10^9–10^{10} infectious units/ml.

For laminin α3 knockdown experiments, MDCK cells were plated for 1.5–2 h on uncoated surfaces until well-attached, gently washed twice with PBS, and infected with virus suspended in a small volume of serum-free Opti-MEM (Invitrogen) for 1 h at 37°C, 5% CO_2. Complete MDCK cell growth medium was then added, and incubation continued. In typical experiments, the multiplicity of infection was 60 infectious units/cell. Under these conditions, knockdown of laminin α3 synthesis, as measured by metabolic labeling, was almost completely effective after 18 h infection. To eliminate any morphogenetic effects of LN5 synthesized before knockdown, infected cultures were most often trypsinized and replated 18 h postinfection.

Cell Proliferation Assay

Cell proliferation was estimated by labeling with BrdU. Control cultures of MDCK cells or cultures infected with either Ad-D5 or Ad-Lac Z for 18 h were trypsinized and replated at low density on glass coverslips and incubated overnight. The next day, cultures were incubated with 50 μM BrdU in complete medium for 6 h. To stain for BrdU, cells were washed, fixed with 3% formaldehyde in PBS, blocked and permeabilized with 5% goat serum and 0.1% Triton X-100 in PBS, and stained with a 1:500 dilution of anti-BrdU in the same blocking buffer supplemented with 20 U of DNAse I (Roche Diagnostics) and 20 mM $MgCl_2$. After washing and staining with a fluorescent secondary antibody, the coverslips were mounted in hard-set Vectashield containing 4,6-diamidino-2-phenylindole (DAPI). Digital micrographs of total (DAPI-stained) nuclei and anti-BrdU-stained nuclei were counted with MetaMorph (Molecular Devices, Sunnyvale, CA), and the fraction of BrdU-positive cells calculated. Labeling experiments were conducted three times with an average of seven fields/treatment (control, Ad-LacZ, and Ad-D5) and 119 cells/field counted.

Wound Healing Assay

Control (uninfected) and Ad-D5– and Ad-LacZ–infected cells were trypsinized and replated on gridded glass coverslips (Bellco Biotechnology, Vineland, NJ). After incubating overnight, approximately one-half of each coverslip was scraped off using a rubber policeman. After changing medium, four regions per coverslip at the wound edge were digitally photographed on an inverted phase microscope at low power, and the cultures incubated for 24 h at 37°C, 5% CO_2. After 24 h, the same regions were rephotographed. To quantitate movement of the wound edge, digital photographs were printed, and the distances measured between fixed points of the grid and the wound edge at the two different time points. Results of three independent experiments with two to four measurements/experiment/treatment condition were averaged.

Analysis of Cell Spreading

Control cultures of MDCK cells or cultures infected with either Ad-D5 or Ad-Lac Z for 18 h were trypsinized and replated at low density on glass

coverslips and incubated overnight. The next day, the cells were fixed and permeabilized, and the actin cytoskeleton visualized with fluorescent phalloidin and the nuclei with DAPI. Total spread area was measured from digital micrographs using phalloidin staining and the threshold setting in MetaMorph. Area/cell was then calculated by counting DAPI-stained nuclei.

Statistical Analysis

Statistical analysis was conducted using Sigma-Stat (SPSS, Chicago, IL) by either the Kruskal–Wallis one-way analysis of variance (ANOVA) on rank with multiple comparisons done by Dunn's test, or by a one-way ANOVA with multiple comparisons carried out by the Holm–Sidak method. Graphs of means + SEs were generated with Sigma-Plot (SPSS).

Sequence Identification

The canine laminin α5 sequence provided here has the EMBL accession no. AY 552590.

RESULTS

MDCK Cells Synthesize LN5 Only When Subconfluent

In the injured kidney, synthesis of LN5 is turned on during regeneration of the epithelium (Zuk and Matlin, 2002). With epithelial cell lines such as MDCK, the equivalent of this regenerative phase is a subconfluent culture, where cells must spread and proliferate to reestablish a continuous epithelium. To determine whether MDCK cells synthesize LN5 under these conditions, cells were plated at low density in uncoated plastic culture dishes. At various times up to 24 h, cells were detached by treatment with Triton X-100 and NH_4OH, and endogenous matrix proteins deposited on the culture dish extracted with SDS. These were then separated by SDS gel electrophoresis and Western blotted with an antibody against the β3 subunit of LN5.

As illustrated in Figure 1A, small amounts of deposited β3 were detectable as little as 6 h after plating, with increasing amounts evident throughout the remaining time points. In addition to the β3 band, another smaller, faint band was also detected with the antibody (Figure 1A, *). This presumably corresponds to a β3 proteolytic fragment.

When such cultures were grown to complete confluence for up to 7 d, and the deposited matrix proteins were examined, the amount of laminin β3 on the culture dish declined by 4 d and was almost undetectable by 7 d (Figure 1B). This suggested that not only was no new LN5 being secreted into the extracellular matrix underlying the cells but also that LN5 deposited earlier was being degraded.

To confirm this, similar cultures on glass coverslips were fixed and stained with a polyclonal antibody against LN5. As shown in Figure 1C, most cells plated for 18 h stained extensively with anti-LN5 antibody (Figure 1C, red) in a dispersed pattern, suggesting that of the endoplasmic reticulum, consistent with continued biosynthesis of LN5. By 4 d of culture, staining was largely absent, being confined to only a few reactive vesicles per cell. By 7 d, staining was almost completely absent (Figure 1C).

To look more directly at the biosynthesis of LN5, cells plated for various times were metabolically labeled for 30 min, and immunoprecipitated LN5 was visualized by fluorography. As shown in Figure 1D, 18 h after plating, all three LN5 subunits, α3, β3, and γ2, were detected. At all other times corresponding to fully confluent cultures, only small amounts of α3 and γ2 were observed, whereas significant quantities of β3 continued to be made. Thus, the decline in LN5 production and deposition observed by Western blotting and immunofluorescence (Figure 1, A–C) was due to differential inhibition of LN5 chain synthesis. Presumably, the β3 chain detected by metabolic labeling in confluent cells (4–10 d after plating; Figure 1D) was degraded in the endoplasmic reticulum and was not secreted in the absence of the other chains because it was not observed at these times by either immunofluorescence (Figure 1C) or Western blotting of deposited matrix proteins (Figure 1B). To determine whether the differential regulation of LN5 chain synthesis was regulated at the transcriptional level, RT-PCR was performed on RNA isolated from subconfluent and confluent cultures. In subconfluent cultures, mRNA for all three chains was detected, whereas only β3 mRNA was found in confluent cultures (our unpublished data).

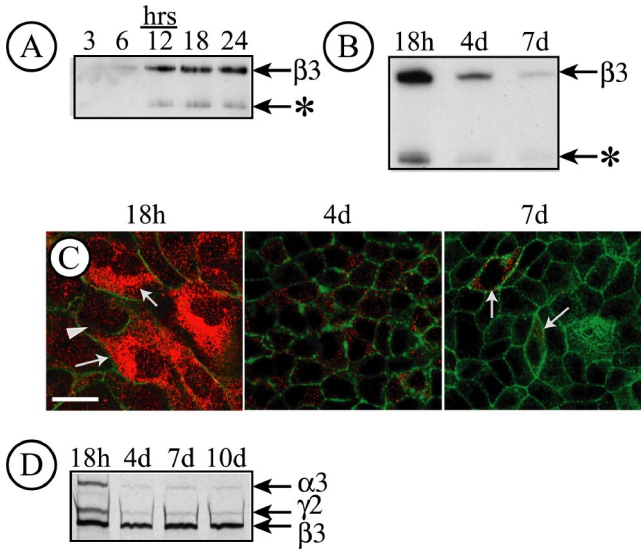

Figure 1. LN5 is only expressed in MDCK cells at early times after plating. (A) Endogenous matrix proteins deposited by MDCK cells (8×10^6 cells/10-cm^2 culture dish) for the indicated times were immunoblotted with an antibody against the laminin β3 subunit. Immunoreactive material corresponding to deposited LN5 was detected beginning at 6 h plating, with increasing amounts afterward. An apparent β3 degradation product was also observed (*). (B) Immunodetection of endogenous matrix proteins deposited on the culture dish by MDCK cells 18 h, 4 d, or 7 d after plating. Under these conditions, LN5 deposition declines significantly after 4 d and is nearly absent after 7 d. As in A, a β3 degradation product is visible (*). (C) MDCK cells (7.5×10^5 cells/35-mm dish) were plated on coverslips and fixed and stained with a polyclonal antibody against LN5 at either 18 h, 4 d, or 7 d after plating. Coverslips were observed by confocal fluorescence microscopy; only sections through the center of the cell are shown. After 18 h, LN5 staining (red) is apparent throughout the cytoplasm in a pattern resembling the endoplasmic reticulum. By 4 d, only a few cytoplasmic vesicles per cell are visible, with only isolated staining (arrows) by 7 d. Green, actin. Bar, 10 μm. (D) Pulse labeling and immunoprecipitation of LN5 in MDCK cells. MDCK cells (1×10^6 cells/35-mm dish) were pulse labeled for 30 min at the indicated times after plating with 50 μCi of [^{35}S]Met/Cys. After labeling, the cells were extracted with RIPA buffer, the extracts were immunoprecipitated with polyclonal anti-LN5, and the immunoprecipitates were analyzed by SDS-gel electrophoresis and fluorography. After 18 h plating, all three LN5 subunits are detected, whereas little α3 or γ2 is detected at later times.

MDCK Cells Also Synthesize at Least One Other Laminin Isoform

Previous studies from other laboratories demonstrated that MDCK cells synthesize laminin, although the particular isoform was not identified (Caplan *et al*., 1987; Boll *et al*., 1991; O'Brien *et al*., 2001). In most, if not all cases, the antibodies used in these studies were made against mouse LN1 (α1β1γ1), and some were specifically reactive with the γ1

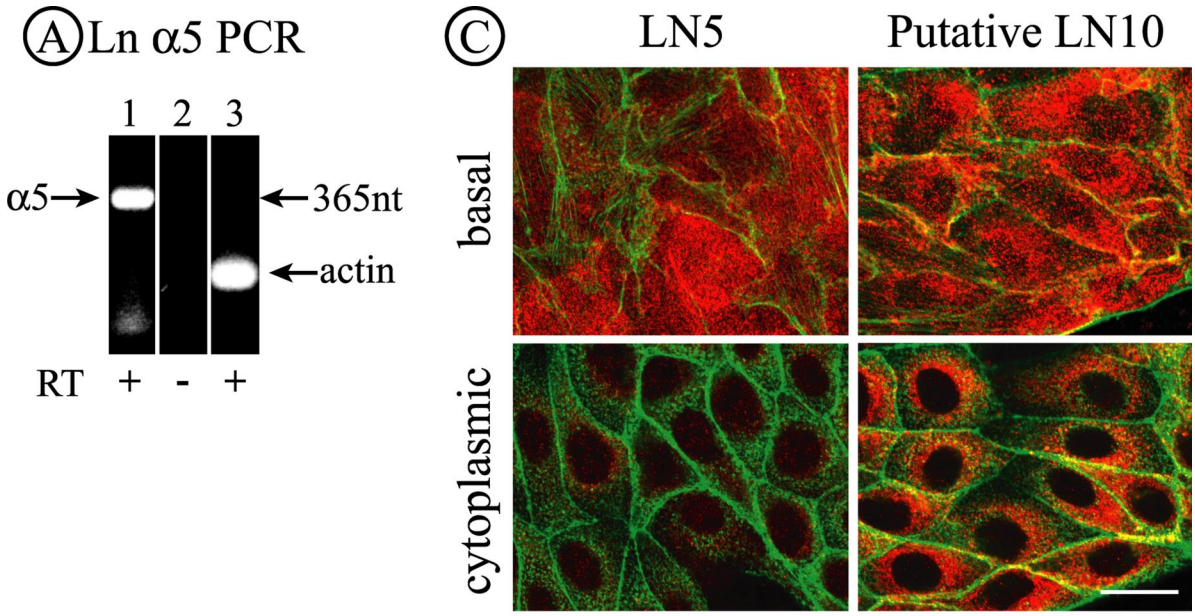

B Comparison of laminin α5 sequences

```
Canine 4     cacctgcccctggatggcttcccctcagcggcgggacccgaggccttgtgtcgtcacgacaacagcctaccccggc 79
Human  3212  cacctccccctggatggcttcccctcggccgccgggctggaggccctgtgtcgccaggacaacagcctgccccggc 3287
Mouse  3212  cacctaccccctggatggcttcccttcagcagctggaactgaggccctgtgtcgccatgacaacagcctgccccggc 3287

Canine 80    cttgccccacggagcaactcagcccctcacatccaccactggccgcctgcctgggcagtgacgtggacgtccagct 155
Human  3288  cctgccccacggagcagctcagcccgtcgcacccgccactgatcacctgcacgggcagtgatgtggacgtccagct 3363
Mouse  3288  cctgccccacagagcagctcagccctcacacccaccgctggcgacctgcttcggcagtgatgtggacatccagct 3363

Canine 156   ccagctggcagtgccacagccaggccgctacgccctggtggtggagtatgccaatgaggacgccccccaggaggtg 231
Human  3364  tcaagtggcagtgccacagccaggccgctatgccctagtggtggagtacgccaatgaggatgcccgccaggaggtg 3439
Mouse  3364  cgagatggccgtgcctcagcctggccaatatgttctcgtggtggaatatgtcggtgaggattcacaccaagagatg 3439

Canine 232   ggcgcagccgtgcacacgccccagcgggccccccagcagggagcactcactttccacccctgccctacagcgccc 307
Human  3440  ggcgtggccgtgcacacccacagcgggccccccagcaggggctgctctccctgcacccctgcctgtacagcaccc 3515
Mouse  3440  ggagtggctgtgcacaccctcagagagccccccagcaaggggtgctcaacctccacccctgcccatacagctccc 3515

Canine 308   tgtgccgggccacagccc 325
Human  3516  tgtgccggggcactgccc 3533
Mouse  3516  tgtgccgg 3523
```

Canine = Human = Mouse
Canine = Human
Canine = Mouse

Figure 2. MDCK cells synthesize the laminin α5 subunit. (A) PCR products corresponding to laminin α5 and β-actin were detected in RNA from MDCK cells by RT-PCR using primers specific to human laminin α5 and canine β-actin. Lanes 1 and 2, laminin α5 primers; lane 3, actin primers. (B) The PCR product shown in A was sequenced and the sequence compared with that of human and mouse laminin α5. The canine sequence is 85% identical to the human sequence and 81% identical to the mouse sequence. (C) MDCK cells (7.5×10^6/35-mm dish) were plated for 42 h and then fixed and stained for either LN5 or putative LN10, the latter using a polyclonal antibody against LN1. Confocal sections from either the extreme base of the cells (top) or through the center of cells (bottom) are illustrated. In the case of LN5, significant amounts of deposited LN5 are visible at the base, but the cytoplasm has only limited amounts of perinuclear staining. For LN10, both the base and cytoplasmic compartments are strongly stained, indicating not only deposition of the protein but also continued synthesis. Bar, 20 μm.

subunit. Because no subunits of LN1 are shared with LN5, it is unlikely that the laminin observed in these previous studies was LN5. However, as at least 10 of the 15 known laminin isoforms contain the γ1 subunit, the identity of this other MDCK cell laminin could not be determined based upon existing data (Miner and Yurchenco, 2004).

Studies of the kidney suggest that LN10 (α5β1γ1) is a prominent isoform in the tubular basement membrane (Miner, 1999). To determine whether MDCK cells, which are of renal origin, express LN10 in addition to LN5, RT-PCR analysis of MDCK RNA was conducted using primers derived from the human laminin α5 sequence. As shown in

Figure 2A, RT-PCR yielded a product of the appropriate size predicted by the human sequence. When sequenced, this product was highly homologous to both the human and mouse laminin α5 sequences, strongly suggesting that this corresponded to the canine homologue (Figure 2B).

As stated previously, polyclonal antibodies against LN1 detect a laminin isoform in MDCK cells. We have also immunoprecipitated a laminin isoform from metabolically labeled MDCK cells with monoclonal anti-γ1 antibody whose subunits correspond in size to a full-size laminin isoform of the type exemplified by both LN1 and LN10 (our unpublished data). Because, RT-PCR of MDCK cell RNA failed to detect laminin α1 mRNA (Yu *et al.*, 2005; our unpublished data), we believe it is likely that the second laminin isoform expressed by MDCK cells is LN10.

To determine whether the synthesis of putative LN10 is regulated the same or differently from LN5, newly confluent cultures of MDCK cells were stained for immunofluorescence with either a polyclonal antibody against LN5 or an antibody prepared against LN1 that reacts with the laminin β1 and γ1 subunits (Yu *et al.*, 2005). The stained samples were examined in the confocal microscope to visualize either the cytoplasmic focal plane or the basal focal plane where deposited matrix molecules can be detected. As illustrated in Figure 2C, under these conditions LN5 staining is present in the basal plane, corresponding to deposited matrix, but nearly absent from the intracellular plane (Figure 2C). In contrast, staining with the anti-LN1 antibody, which presumably detects LN10, is evident both on the basal surface and intracellularly (Figure 2C). Thus, synthesis of LN5 and putative LN10 are clearly induced at different times during MDCK cell morphogenesis.

MDCK Cells Use Two Different Integrins to Attach to and Spread on LN5

Keratinocytes and other epithelial cell types have been shown to attach to LN5 via the integrins $\alpha3\beta1$ and $\alpha6\beta4$ (Niessen *et al.*, 1994; Kreidberg, 2000; Kreidberg and Symons, 2000; Nguyen *et al.*, 2001). MDCK cells express both of these integrins as well as $\alpha2\beta1$ and $\alpha V\beta3$ (Schoenenberger *et al.*, 1994). To determine which integrins MDCK cells use for adhesion to LN5, purified LN5 was coated on microtiter plates and adhesion of MDCK cells measured after 90 min in the presence or absence of function-blocking anti-integrin antibodies. As shown in Figure 3, MDCK cells attached readily to wells coated with collagen I to an extent corresponding to nearly 100% adhesion of the applied cells (our unpublished data). Adhesion to collagen was completely inhibited by treatment of cells before assay with a function-blocking anti-β1 integrin antibody, AIIB2, indicating that it is mediated by β1 integrins (Figure 3). Cells added to wells coated with purified LN5 adhered to the same extent as to collagen (Figure 3). However, in contrast to collagen, anti-β1 had no effect on adhesion to LN5 (Figure 3). A function-blocking antibody against the integrin α6 subunit, GoH3, inhibited adhesion of MDCK cells to LN5 by ~33% (Figure 3). However, when GoH3 and AIIB2 were combined, inhibition increased to about two-thirds (Figure 3), suggesting that both β1- and α6-containing integrin receptors are involved in MDCK cell adhesion to LN5.

To determine why the anti-β1 integrin antibody alone did not affect adhesion to LN5, cells treated with either AIIB2 or GoH3 were plated on glass coverslips coated with LN5, and their morphology was compared with untreated cells plated on coverslips coated with either collagen I or LN5 by Nomarski differential interference contrast (DIC) microscopy. On collagen, cells were asymmetrically spread, with some exhibiting an extended lamellipodium from one side (Figure 4A, i). When plated on a LN5 coated surface, cells were extensively and symmetrically spread (Figure 4A, ii). Staining of such cells with fluorescent phalloidin revealed uncharacteristic thick bundles of filamentous actin at the periphery of the round cells (Figure 4A, ii, inset). When cells were treated with anti-β1 integrin antibody before plating on LN5, they still attached readily, but they failed to spread, often exhibiting small blebs at the edge of the cell (Figure 4A, iii, arrowheads). When treated instead with anti-α6 integrin antibody, cells still spread on LN5, but not to the same extent as untreated cells, and had a subtly changed, less uniform cytoplasmic morphology by DIC microscopy (Figure 4A, iv). In separate experiments, quantitation of spreading by MDCK cells plated on uncoated glass, or coverslips coated with either collagen I or LN5 confirmed that LN5 induced significantly more spreading than the other two surfaces (Figure 4B).

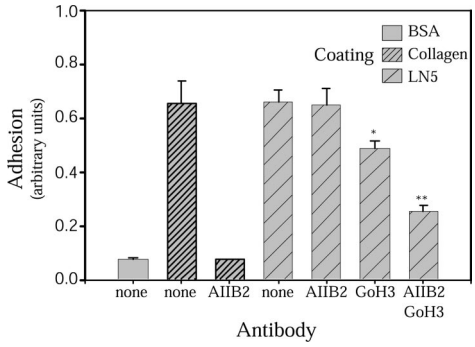

Figure 3. MDCK cells use β1 integrins and $\alpha6\beta4$ integrin to adhere to LN5. A single-cell suspension of MDCK cells was plated in wells of a 96-well plate coated with either bovine serum albumin (BSA) (−control), collagen I, or LN5 in the presence or absence of function-blocking antibodies against β1 integrin (AIIB2) or α6 integrin (GoH3). After 90-min incubation at 37°C, unattached cells were washed away, and numbers of attached cells were estimated after fixation and staining by measuring absorbance of solubilized stain. Almost no cells attach to BSA-coated wells, whereas nearly all cells attach to wells coated with either collagen I or LN5. Anti-β1 integrin abolishes all adhesion to collagen I, but by itself has no effect on adhesion to LN5. Anti-α6 integrin reduces cell adhesion to LN5 somewhat, but is much more effective in combination with anti-β1 integrin. *$p < 0.05$ and **$p < 0.001$ relative to no antibody LN5 control.

Based upon these findings, it seems clear that MDCK cells, like other epithelial cells, use both a β1 integrin and integrin $\alpha6\beta4$ to bind to LN5. MDCK cells do not express $\alpha6\beta1$(Schoenenberger *et al.*, 1994). Furthermore, the β1 integrin is likely responsible for spreading of MDCK cells over LN5 coated surfaces, because antibody blocking of β1 integrins prevents spreading but not adhesion (Figure 4A, iii).

Inhibition of Laminin α3 Synthesis with siRNA

To investigate further the function of LN5 in MDCK cell morphogenesis, LN5 synthesis was disrupted by expression of a siRNA targeted to the laminin α3 subunit (Elbashir *et al.*, 2001, 2002). In preliminary experiments, a synthetic RNA duplex based on the canine α3 sequence was transiently transfected into MDCK cells. A control RNA duplex was also transfected. As shown in Figure 5A, transfection of RNA targeted to laminin α3 eliminates mRNA detectable by RT-PCR, whereas transfection of the control RNA or the transfection reagent alone had no effect.

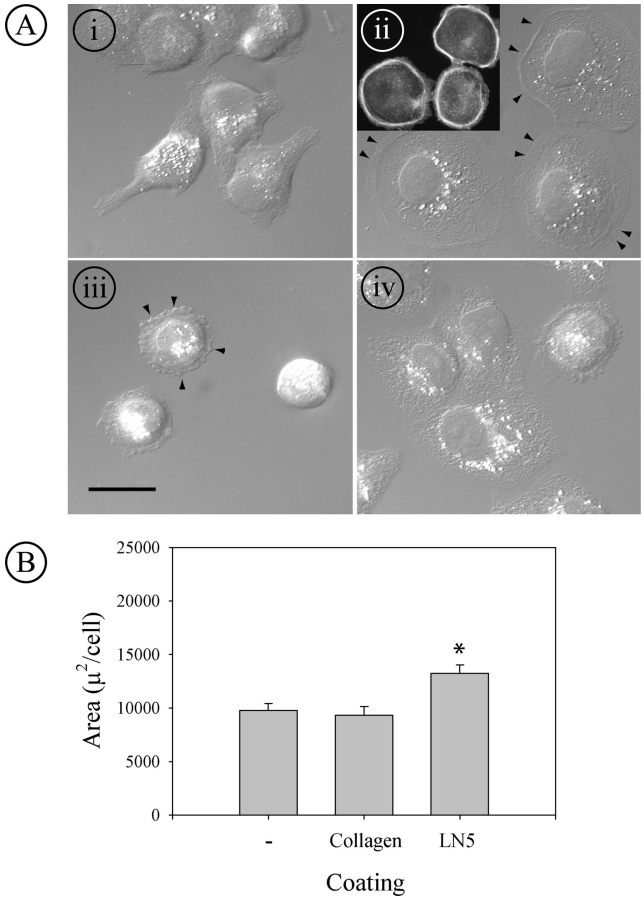

Figure 4. MDCK cells spread extensively on LN5 using a β1 integrin. (A) MDCK cells were plated on coverslips coated with collagen I (i) or LN5 (ii–iv) for 2 h at 37°C in the presence or absence of function-blocking anti-β1 integrin (AIIB2; iii) or α6 integrin (GoH3; iv). At the end of the incubation, the cells were fixed and stained with fluorescent phalloidin and viewed by Nomarski DIC microscopy (i–iv) or fluorescence microscopy (ii; inset). On collagen, cells spread asymmetrically and extend narrow lamellipodia (i); on LN5, cells spread more extensively and symmetrically than on collagen (ii; arrowheads mark cell edges). By fluorescence, the spread cells on LN5 display thick bundles of filamentous actin at the cell periphery (ii; inset). In the presence of anti-β1 integrin, cells attach to LN5 but do not spread, and blebs are present at the cell peripheries (arrowheads; iii). In the presence of anti-α6 integrin, the cells on LN5 spread but not as extensively or uniformly as in the absence of antibody (iv). Bar, 10 μm. (B) MDCK cells were plated at subconfluent density for 24 h at 37°C on uncoated glass coverslips or coverslips coated with either collagen I or LN5. At the end of the incubation, the cells were fixed and stained with fluorescent phalloidin and DAPI. The area occupied by spread cells was then measured using MetaMorph. Cells plated on LN5 spread significantly more than those plated on either glass or collagen I. *$p < 0.001$ relative to uncoated control and collagen coating.

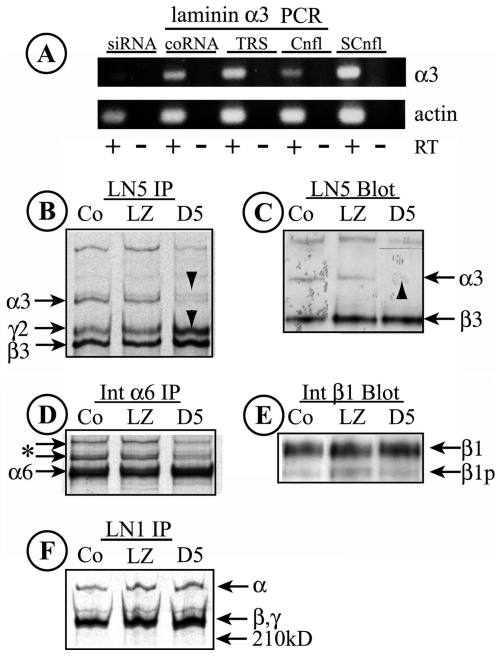

Figure 5. Knockdown of laminin α3 with siRNA. (A) RNA was harvested from MDCK cells transfected for 2 d with either a synthetic RNA duplex specific for a target sequence in canine laminin α3 (siRNA), a control duplex not representing any known gene (coRNA), or transfection reagent alone (TRS). RNA was also harvested from confluent (Cnfl) or subconfluent (SCnfl) MDCK cell cultures. Laminin α3 and actin transcripts were detected by RT-PCR. RT, reverse transcriptase added to the reaction. Note the absence of a laminin α3 band with transfected siRNA. (B) LN5 was immunoprecipitated from detergent extracts of metabolically labeled control MDCK cells (Co) or cells infected with siRNA-expressing adenovirus (D5) or a control virus (LZ). In both Co and LZ samples, all three LN5 bands are visible; in the D5 siRNA sample, little laminin α3 can be seen, whereas the levels of laminin β3 and γ2 chains are increased (arrowheads). (C) Extracts from control (Co), Ad-LacZ–infected, and Ad-D5–infected MDCK cells were immunoblotted with anti-LN5. Laminin α3, which is weakly detected by the antibody, is absent in cells expressing siRNA (arrowhead). The laminin γ2 chain is not detected by the antibody. (D and F) The labeled cell extracts used to immunoprecipitate LN5 in B were sequentially immunoprecipitated with anti-α6 integrin (D) and anti-LN1 (F). No significant differences between the samples are evident, suggesting that siRNA-mediated knockdown of laminin α3 is specific. The two bands in D running more slowly than α6 (* and arrows) are unidentified but may correspond to forms of integrin β4. In F, the higher molecular weight band is likely laminin α5 and the lower doublet β1 and γ1. (E) The immunoblot shown in C was stripped and reprobed with anti-β1 integrin. No significant differences between samples can be seen. β1, mature β1 integrin; β1p, precursor β1.

For additional experiments, the RNA sequence against the target was engineered as a short hairpin in an adenoviral vector, and an adenovirus stock was prepared. When this "D5" stock was used to infect MDCK cells, and LN5 immunoprecipitated with a polyclonal antibody from metabolically labeled cells, the α3 band was almost completely absent (Figure 5B, arrowhead, D5 lane). In contrast, α3 was readily detected in immunoprecipitates from control (noninfected, Co) cells and cells infected with an adenoviral vector expressing LacZ (Figure 5B, LZ). Strikingly, increased amounts of both β3 and γ2 chains were present in the labeled samples (Figure 5B, D5, arrowhead), suggesting that the knockdown of laminin α3 synthesis leads to either the relative accumulation of the other LN5 chains in the endoplasmic reticulum or to their increased synthesis.

Similarly, when extracts from D5-infected, LZ-infected, and noninfected cells were immunoblotted with the same antibody, no α3 band was detected (Figure 5C, note that the antibody does not react with γ2). Under these conditions, the intensity of the β3 band did not change significantly upon knockdown, indicating that the steady-state levels of β3 as detected by Western blotting were not detectably changed by reduction in the α3 chain (Figure 5C).

Knockdown of laminin α3 seemed to be specific. In addition to the continued expression of the other LN5 chains, there were little or no differences between control, LZ, or D5 samples in the amounts of integrin α6 or presumptive LN10 immunoprecipitated from metabolically labeled cells (Figure 5, D and F), or in the amount of integrin β1 detected by Western blotting of cell extracts (Figure 5E).

Knockdown of Laminin α3 Affects Cell Spreading

Based upon the observation that plating of normal MDCK cells on surfaces coated with LN5 led to extensive cell spreading, our expectation was that knockdown of laminin α3 and the resulting disruption of LN5 production would yield cells unable to spread effectively. Instead, when cells were infected overnight with the D5 virus, and then replated on uncoated surfaces, they spread much more extensively than either uninfected control cells or cells infected with the LacZ-expressing virus, yielding round, flat cells resembling fried eggs (Figure 6A). Spreading was so extreme that nuclei were flattened, looking enlarged, and was apparently facilitated by extensive formation of actin stress fibers (Figure 6A, arrows). The amount of spreading also did not seem to be affected by the formation of cell–cell contacts (Figure 6A, Ad-D5, inset). Quantitation of spreading indicated that cells with α3 synthesis knocked down occupied, on average, three times more area than either control group (Figure 6B).

To determine whether exogenous LN5 would cause the unusual "fried egg" phenotype to revert to normal spreading, uninfected, Ad-LacZ–infected, and Ad-D5–infected cells were plated on glass coverslips coated with purified human LN5, and the spread areas were measured. As shown in Figure 6B, plating on LN5 induced increased spreading of uninfected and Ad-LacZ–infected cells relative to uncoated controls (Figure 4B). However, plating of the Ad-D5 cells on LN5 *further increased* spreading relative to not only controls (2.7-fold) but also relative to D5 cells plated on uncoated surfaces (1.6-fold).

Based upon these observations, we conclude that LN5 does not simply induce spreading of cells but also may regulate spreading in a manner that cannot be duplicated by exogenous LN5. Indeed, provision of exogenous LN5 seems to further exacerbate the dysregulation of cell spreading.

Inhibition of Laminin α3 Synthesis Leads to Secretion of Laminin β3 and γ2

When uninfected control cells and Ad-LacZ–infected cells were stained with polyclonal anti-LN5 and examined in the confocal microscope, deposition of LN5 was observed under the cells in a typical uneven pattern with the largest amounts tending to occur near the edges of multicell islands (Figure 7A). Cells infected with Ad-D5, in which laminin α3 synthesis is knocked down, also deposit antibody-reactive material on the substratum. However, the pattern of this deposition, although still uneven, often is whorled to resemble a rose blossom. This pattern may result from circular movement of cells as they deposit the proteins on the substratum (Aumailley, personal communication). Because the anti-LN5 antibody used for immunofluorescence strongly reacts with laminin β3 and is apparently less reactive with canine laminin α3 (Figure 5C), it was impossible to determine whether this pattern was caused by residual heterotrimeric LN5 secreted before knockdown was complete, or secreted laminin β3, possibly in a dimeric complex with γ2 (Hirosaki *et al.*, 2000).

To examine this, control uninfected cells and cells infected with Ad-LacZ and Ad-D5 overnight were replated for 24 h and then metabolically labeled overnight. After this, both

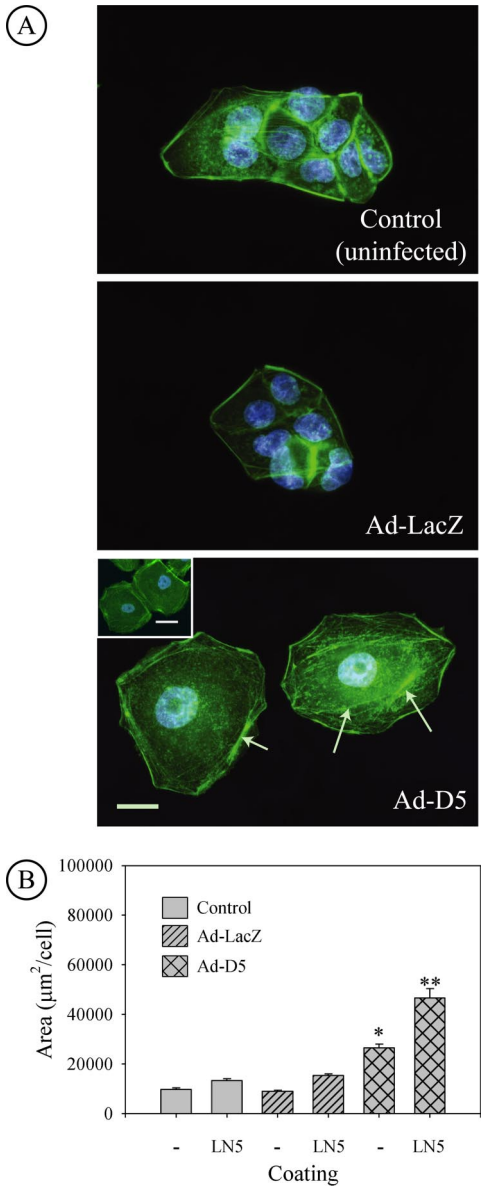

Figure 6. Knockdown of laminin α3 leads to increased spreading of MDCK cells. (A) Uninfected MDCK cells and cells infected with control Ad-LacZ virus or siRNA-expressing Ad-D5 virus were replated on uncoated glass coverslips overnight and then fixed and stained with fluorescent phalloidin (green) and DAPI (blue) to visualize the actin cytoskeleton and nuclei, respectively. Micrographs show that cells infected with Ad-D5 spread much more than either control or Ad-LacZ–infected cells and are so flat that the nucleus is distorted and seems larger. Bundles of actin filaments and extensive actin stress fibers are also apparent (arrows). Bar, 20 μm. Inset in Ad-D5 panel, formation of cell–cell contacts does not suppress extensive cell spreading. Bar, 20 μm. (B) Control MDCK cells or cells infected with Ad-LacZ or Ad-D5 were replated on uncoated glass coverslips (−) or coverslips coated with purified human LN5 (LN5). Fixed cells were stained with fluorescence phalloidin and DAPI, and spread area/cell was measured from digital micrographs. Cells expressing siRNA targeted against laminin α3 spread much more than either control or Ad-LacZ–infected cells. Spreading of all cells is stimulated further by plating on LN5-coated coverslips. *$p < 0.05$ relative to uncoated control and Ad-LacZ. **$p < 0.05$ relative to LN5-coated control and Ad-LacZ replated on LN5. Ad-D5 on uncoated glass (*) compared with Ad-D5 on LN5-coated glass (**$p < 0.001$ by *t* test).

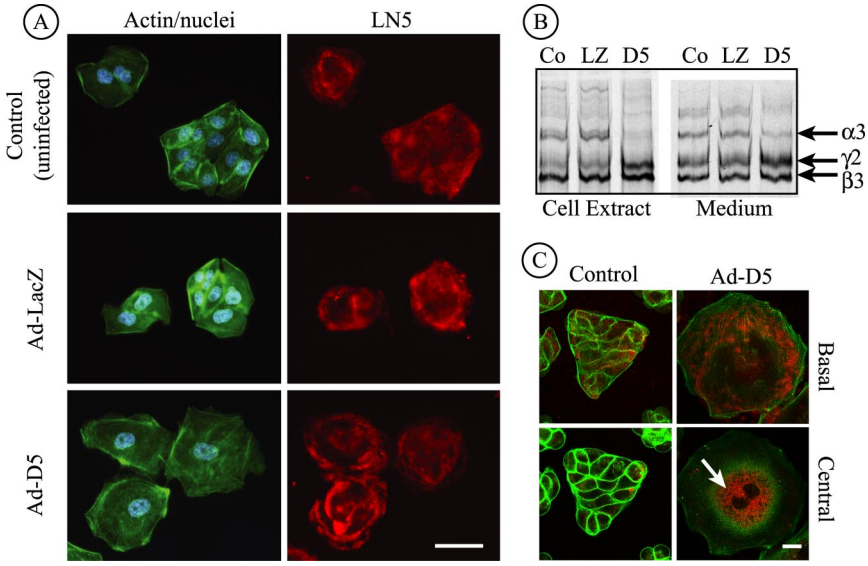

Figure 7. Laminin β3 and γ2 are secreted after siRNA-mediated knockdown of laminin α3. (A) Control MDCK cells or cells infected for 18 h with Ad-LacZ or Ad-D5 were replated on uncoated glass coverslips for 24 h and stained with antibodies against LN5 (red), fluorescent phalloidin (green), and DAPI (blue), and viewed by conventional immunofluorescence microscopy. Anti-LN5 antibody staining is visible at the base in all three cases, although the staining pattern under cells expressing siRNA (Ad-D5) exhibits a characteristic "rose petal" pattern. Bar, 20 μm. (B) Control MDCK cells or cells infected with Ad-LacZ or Ad-D5 were metabolically labeled overnight. Detergent cell extracts and culture medium were immunoprecipitated with anti-LN5, and precipitated polypeptides were visualized on SDS-gels by fluorography. In extracts from Ad-D5–infected cells, the laminin α3 band is absent and laminin β3 and γ2 are increased in intensity (D5 lane). In the medium, laminin α3 is detectable but diminished, and the ratio of the β3 and γ2 bands to α3 is higher than controls, suggesting secretion of β3 and γ2 uncomplexed to α3 (compare D5 with Co and LZ). (C) Control MDCK cells or cells infected for 42 h with Ad-D5 were replated on uncoated glass coverslips for 24 h, stained with antibodies against LN5 (red) and fluorescent phalloidin (green), and viewed by confocal fluorescence microscopy. Individual optical sections taken at either the base of the cells or through the cell center are shown. Cells infected with Ad-D5 are exceedingly spread and still exhibit some staining with anti-LN5 at the base of the cell. Inside the same cells, anti-LN5 staining is intense in what seems to be the endoplasmic reticulum (arrow). Control (uninfected) cells seem normal with some anti-LN5 staining both within the cell and at the cell base. Ad-LacZ–infected cells seemed identical to uninfected controls (our unpublished data). Bar, 10 μm.

the culture medium and cell extracts were immunoprecipitated with anti-LN5 antibody. As shown in Figure 7B, little or no labeled laminin α3 is present in Ad-D5–infected cells at the time of extraction relative to controls, and both the β3 and γ2 chains have accumulated in the cell to an abnormal extent (Figure 5B). In the medium, all three LN5 chains are evident in both knockdown cells and controls. In Ad-D5 cells, however, the amount of laminin α3 is significantly reduced relative to the other chains in the same cells and in controls, and the amounts of both β3 and γ2 are increased relative to controls. This clearly suggests that, at the time examined, Ad-D5 cells secrete not only some residual heterotrimeric LN5 but also both β3 and γ2 chains.

Because these experiments indicated that the Ad-D5–induced knockdown was incomplete in the time period tested, infected cells were incubated an additional 24 h, and LN5 was visualized by immunofluorescence and confocal microscopy. As shown in Figure 7C, Ad-D5–infected cells continued to spread even further relative to control cells as incubation was continued, providing additional evidence that knockdown of laminin α3 leads to dysregulation of spreading (Figure 7C, basal image). Under these conditions, deposited immunoreactive material was still apparent, but it was somewhat diminished and spotty relative to earlier times (Figure 7A). In confocal optical sections traversing the cytoplasm, extensive bright staining with the LN5 antibody was observed, apparently corresponding to the endoplasmic reticulum engorged with the β3 and γ2 chains.

On the basis of these experiments, we believe that knockdown of laminin α3 likely leads to secretion and deposition of the other LN5 chains. This secretion, however, seemed somewhat inefficient, leading to their accumulation in the endoplasmic reticulum. Although it is likely that secreted β3 and γ2 are present in a heterodimeric complex (Kariya *et al*., 2002), this cannot be ascertained definitively with the current data.

Knockdown of Laminin α3 Inhibits Proliferation and Wound-Edge Migration

A previous study used function-blocking antibodies against LN5 to demonstrate that LN5 stimulated cell proliferation (Gonzales *et al*., 1999). To determine whether this was also the case in MDCK cells in which synthesis of laminin α3 was suppressed, MDCK cells infected with the D5 adenovirus or the LacZ adenovirus, or noninfected control cells, were replated at equal subconfluent densities onto uncoated coverslips and labeled with BrdU for 6 h. Afterward, cultures were fixed and stained with a specific antibody against BrdU and DAPI to mark all nuclei, and the fraction of positive nuclei scored by fluorescence microscopy. As shown in Figure 8, both control cells and cells infected with the LacZ

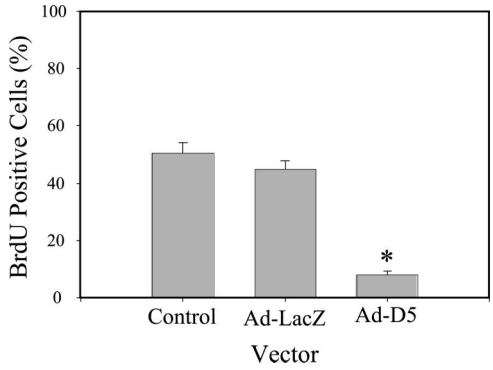

Figure 8. Knockdown of laminin α3 blocks proliferation. Control MDCK cells or cells infected for 18 h with Ad-LacZ or Ad-D5 were replated on uncoated glass coverslips for 24 h, incubated with BrdU for 6 h, stained with antibodies against BrdU and DAPI (blue), and viewed by conventional immunofluorescence microscopy. Proliferation was measured by counting total and BrdU-positive nuclei. *$p < 0.05$.

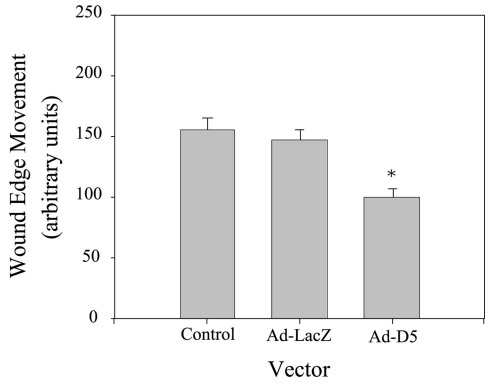

Figure 9. Knockdown of laminin α3 slows wound-edge migration. Control MDCK cells or cells infected for 18 h with Ad-LacZ or Ad-D5 were replated at confluent density on gridded, uncoated glass coverslips for 24 h, and wounded by scraping. Wound-edge migration relative to the time of wounding was measured on micrographs after 24 h. Note that wound-edge movement occurred under all three conditions but was significantly reduced in cells expressing siRNA (Ad-D5). *$p < 0.05$.

virus incorporated BrdU into ~50% of their nuclei, whereas D5-infected cell nuclei were <10% BrdU positive. Clearly, knockdown of laminin α3 synthesis and its resulting effects on LN5 production block cell proliferation.

LN5 plays an important role in wound healing in the skin and has also been implicated in the migration of a variety of other cells (Zhang and Kramer, 1996; Giannelli *et al*., 1997; Goldfinger *et al*., 1998; Decline and Rousselle, 2000; Koshikawa *et al*., 2000; Frank and Carter, 2004; Hintermann and Quaranta, 2004). Furthermore, its expression in the kidney after ischemic injury occurs at a time when the restoration of an intact epithelium occurs. To test the involvement of LN5 in processes related to wound healing in MDCK cells, we replated cells infected with either D5 or control adenoviruses, or noninfected control cells, on uncoated, gridded coverslips at confluent density. The next day, the resulting monolayer was wounded by scraping, and migration of the wound edge then measured after 24 h. Under these conditions, the wound edge of both control and LacZ virus-infected cells migrated approximately the same distance in 24 h (Figure 9). In contrast, the extent of movement of the D5 cells was significantly less than controls, suggesting that LN5 is important in MDCK cell wound healing (Figure 9).

Knockdown of Laminin α3 Does Not Affect Apical–Basal Polarization of the MDCK Cell Epithelium

As described in the introduction, laminin has been implicated in epithelial cell polarization (Klein *et al*., 1988; Zinkl *et al*., 1996; Li *et al*., 2003; Miner and Yurchenco, 2004). The synthesis of LN5 seems to be confined mainly to the period before and perhaps just after the formation of a complete epithelium. Nevertheless, it was possible that it still plays an essential role in generating apical–basal polarity, either by directly signaling to the cells setting up the epithelium, or by influencing the assembly of a nascent basal lamina that, in turn, provides essential polarization signals. To determine whether LN5 is involved in apical–basal polarization of MDCK cells, control, noninfected cells and cells infected with the D5 adenovirus or LacZ adenovirus were plated at near confluent density on uncoated permeable supports and cultured overnight. Under these conditions, MDCK cells are known to polarize with respect to specific apical and basolateral antigens by 18 h. Polarization and overall organization was then assessed by confocal immunofluorescence microscopy using antibodies against the apical marker gp135 and the basolateral protein E-cadherin, and fluorescent phalloidin to stain the actin cytoskeleton.

As shown in Figure 10, both control and LacZ adenovirus-infected cells formed uniform monolayers that were completely polarized relative to apical (Figure 10A) and basolateral (Figure 10B) proteins. The monolayer formed by the D5 adenovirus-infected cells, although generally intact, was very heterogeneous in cell size and shape. Nevertheless, apical and basolateral proteins were still segregated to the appropriate plasma membrane domains.

DISCUSSION

Our results demonstrate that MDCK cells synthesize and deposit LN5 while reconstituting a confluent epithelium, and then they turn off its synthesis upon reaching confluence. We also show that MDCK cells spread more extensively on surfaces coated with exogenous LN5 than on either an uncoated surface or a surface coated with collagen I, and, like other epithelial cells, they interact with LN5 through a β1 integrin and integrin α6β4. The β1 integrin, which is likely α3β1, is largely responsible for cell spreading, because a function-blocking anti-β1 integrin antibody prevents spreading but not cell adhesion.

Through the inhibition of laminin α3 synthesis using siRNA, we have also uncovered additional clues to the functions of LN5 in MDCK cells. On knockdown of laminin

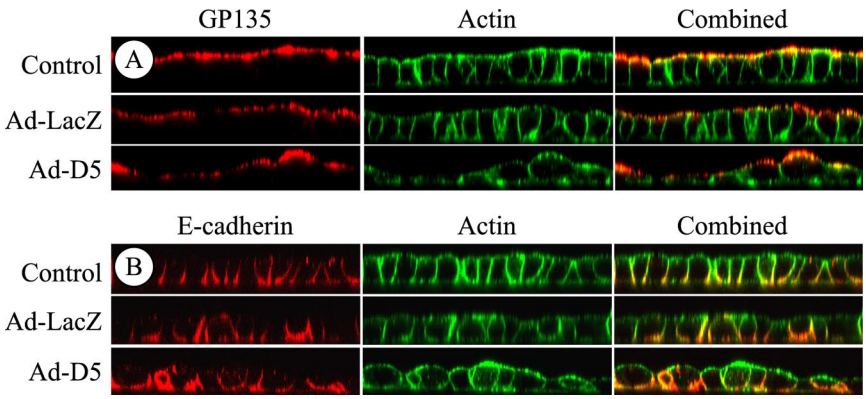

Figure 10. Knockdown of laminin α3 affects epithelial morphogenesis but not apical–basal polarization. Control MDCK cells or cells infected for 18 h with Ad-LacZ or Ad-D5 were replated at confluent density on uncoated Transwell supports for 24 h and stained with antibodies against either the apical antigen gp135 (A; red) or the basolateral protein E-cadherin (B; red) and fluorescent phalloidin (green). The stained samples were imaged as orthogonal Z-sections by confocal fluorescence microscopy. Note that the epithelium formed by Ad-D5–infected cells is heteromorphic with cells of different sizes and shapes, but it is as polarized relative to both apical and basolateral proteins as control and Ad-LacZ–infected cultures. Cell height in all samples is ~10–15 μm.

α3, MDCK cells spread more rather than less, and this behavior is not suppressed but rather stimulated upon plating on exogenous LN5. Furthermore, in agreement with previous studies (Gonzales *et al*., 1999), our results indicate that suppression of LN5 production severely inhibits cell proliferation and reduces wound-edge migration, possibly as a partial consequence of the proliferation block. Finally, we show that LN5 is not critically required for apical–basal polarization of MDCK cells, at least in monolayer cultures, despite significant disruption of normal morphogenesis.

Regulated Synthesis of LN5

Our observation that LN5 synthesis only occurs in subconfluent MDCK cells is novel, and, to our knowledge, it has not been reported for other LN5-producing cell lines. These results with MDCK cells closely parallel our previous observation that LN5, which is not expressed to any great extent in the normal adult kidney, is strongly induced in the rat kidney after ischemic injury (Zuk and Matlin, 2002). In that instance, increased LN5 production occurs 24–48 h after injury at the beginning of the period in which the tubular epithelium regenerates. Thus, the implication of both our in vitro results with MDCK cells and our previous in vivo findings is that LN5 is a key participant in the reestablishment of a continuous epithelium. Induction of LN5 has also been reported in human polycystic kidney epithelium, suggesting, perhaps, that LN5 plays a role in the pathogenesis of the disease by causing tubular epithelial cells to be locked in a chronically regenerative state (Joly *et al*., 2003).

Pulse-labeling experiments indicate that the shutdown of LN5 synthesis may occur by blocking either the transcription or translation of mRNA for the α3 and γ2 chains without affecting β3 synthesis. A similar mechanism for regulation of LN5 production may also function in keratinocytes as well as normal and ras-transformed HaCat cells (Aumailley, personal communication; Korang *et al*., 1995). In addition, this unusual regulatory scheme was previously observed in the normal human mammary epithelial cell line MCF-10A stably overexpressing the p300 transcriptional coactivator (Miller *et al*., 2000). Under normal conditions, MCF-10A cells constitutively express LN5. When p300 is overexpressed, however, mRNAs for laminin α3 and γ2 are significantly decreased, whereas the message for β3 is not, paralleling our results with MDCK cells. Although there is no evidence that p300 is involved in the regulation of transcription after kidney injury or in MDCK cells, its ubiquitous expression certainly makes it a possibility.

LN5 has been previously implicated in the healing of cutaneous wounds (Decline and Rousselle, 2000; Nguyen *et al*., 2000b, 2001; Aumailley *et al*., 2003; Frank and Carter, 2004). In the epidermis, however, LN5 not only plays a transient role in wound healing but also is a constitutive structural component linking the epidermis to the dermis. On wounding, LN5 synthesis increases, and its deposition facilitates healing by regulating cell migration and reassembly of the basal lamina. In contrast to the skin, what is unique about MDCK cells is that LN5 is completely removed from the substratum shortly after synthesis ceases. How this occurs is not known, but it may involve matrix metalloproteinases. Based upon our observations, it will be of interest to examine other cell types and tissues not previously suspected of making LN5 to determine whether it plays a discrete role during regeneration after injury, with the evidence of its function then destroyed by degradation.

LN5 secreted from MDCK cells has α3, β3, and γ2 chains of approximately 200, 140, and 155 kDa, respectively. These are essentially identical in size to the chains immunoprecipitated from extracts of MDCK cells, suggesting that little or no proteolytic processing occurs upon secretion. In the postischemic rat kidney, we also observed that the laminin α3 chain was not proteolytically processed. LN5 in mature, quiescent skin as well as that found in conditioned culture medium from human keratinocytes is predominantly composed of α3 and γ2 chains processed to 165 and 105 kDa, respectively (Marinkovich *et al*., 1992; Nguyen *et al*., 2000b; Aumailley *et al*., 2003). In wounded skin, keratinocytes at the wound edge are stimulated to secrete "precursor" LN5 resembling that seen in MDCK cells (Nguyen *et al*., 2000b). This form of LN5 is considered to be promigratory, whereas LN5 with processed α3 and unprocessed γ2 is thought to stimulate more stable adhesion (Ghosh and Stack, 2000). Given that LN5 only occurs in MDCK cells and the postischemic kidney in association with reformation of the intact epithelium, our results are consistent with these interpretations.

LN5 and the Regulation of Cell Spreading

Knockdown of laminin α3 using siRNA led to extensive spreading of MDCK cells plated on uncoated surfaces. When such cells were plated on surfaces coated with exogenous LN5, the spreading phenotype was not reversed, but enhanced (Figure 6). Although these surprising results are difficult to explain at this time, several factors are worth considering.

Matrix proteins other than LN5 may contribute to excessive cell spreading in the knockdown cells. In the experiments described here, MDCK cells in which laminin α3 was suppressed were replated in FBS-containing medium on either uncoated surfaces or surfaces coated with LN5. Serum may provide sufficient fibronectin or vitronectin (or both) to ligate integrin αVβ3 in MDCK cells and cluster it in basal adhesion complexes (Waechter and Matlin, unpublished data). In addition, we cannot exclude aberrant effects of other matrix proteins, such as collagen IV, LN10, or proteoglycans, on cell spreading in the absence of LN5. It is possible that one of the functions of LN5 is to modulate the activities of other integrins such as αVβ3, and, in the absence of LN5, these integrins and their associated proteins promote uncontrolled spreading.

Recent observations with keratinocytes expressing a β4 integrin mutant are consistent with this interpretation (Nikolopoulos *et al*., 2005). Primary keratinocytes from a mouse homozygous for β4 integrin deleted in the substrate domain of the carboxy-terminal cytoplasmic tail spread more extensively than wild-type cells when plated on LN5 in serum-free conditions. They also exhibited reduced wound closure when stimulated with epidermal growth factor and serum. From this, it was concluded that the β4 integrin substrate domain opposes spreading stimulated by LN5 ligation of α3β1. Previous studies have also proposed that α6β4 integrin exerts such a "transdominant" inhibitory effect on α3β1 integrin in keratinocytes on LN5 (Nguyen *et al*., 2000a, b, 2001). Similarly, in MDCK cells, α6β4 interacting with LN5 might also oppose cell spreading stimulated by α3β1; in the absence of LN5 but in the presence of serum factors, both α6β4 and α3β1 would be disengaged rendering α6β4 unable to restrain spreading promoted by αVβ3.

Although it is puzzling that provision of exogenous LN5 stimulated additional spreading of the knockdown-MDCK cells instead of reversion of the spread phenotype, it is important to keep in mind that the LN5 used for coating was derived from keratinocyte-conditioned medium and therefore proteolytically processed (Aumailley *et al*., 2003). Although processing of α3 alone is believed to yield LN5 that

promotes adhesion rather than migration, processing of γ2 in addition to α3, as occurs in keratinocytes, again renders LN5 promigratory (Ghosh and Stack, 2000). Indeed, processed γ2 and the resulting peptides are widely considered to be markers of metastatic and invasive carcinomas (Giannelli and Antonaci, 2000).

A number of previous studies have implicated LN5 in cell migration (Zhang and Kramer, 1996; O'Toole *et al*., 1997; Goldfinger *et al*., 1998; Ghosh and Stack, 2000; Nguyen *et al*., 2000a, b, 2001; Frank and Carter, 2004; Hintermann and Quaranta, 2004). Although at first glance some of this literature seems contradictory, with LN5 postulated to be either promigratory or proadhesive (that is, antimigratory), an appropriate general conclusion may be that LN5 regulates cell migration by not only directly affecting adhesion complexes involving its own integrin receptors α3β1 and α6β4 but also by damping or stimulating the activities of other adhesion receptors ligated to matrix components such as collagens, fibronectin, and even vitronectin. Furthermore, each of these activities is likely modulated to varying extents by proteolytic processing of the α3 and γ2 laminin chains (Ghosh and Stack, 2000). Ideas similar to these have been previously proposed in relation to keratinocyte migration and the healing of cutaneous wounds, in particular (Nguyen *et al*., 2000b).

At this time, it is unknown which signaling pathways might be implicated in the stimulated spreading of MDCK cells that occurs upon knockdown of laminin α3 expression. An obvious possibility is the Rho-GTPase family (Jaffe and Hall, 2005). In particular, Rac1 affects the formation of lamellipodia and focal complexes, whereas RhoA regulates the formation of focal adhesions and stress fibers. Nevertheless, preliminary experiments in our laboratory suggest that knockdown of laminin α3 does not particularly stimulate the activity of Rac1, RhoA, or Cdc42 relative to controls (Buschmann, Waechter, and Matlin, unpublished data). Furthermore, expression of dominant-negative Rac1 or RhoA in MDCK cells does not suppress the spread phenotype (Buschmann, Waechter, and Matlin, unpublished data). Other recent experiments, however, have detected differences in the tyrosine phosphorylation of some unidentified proteins that might be implicated in the spreading phenotype. Future experiments will explore the apparent dysregulation of signaling caused by laminin α3 knockdown in more detail.

LN5 and Cell Proliferation

In our experiments, proliferation of MDCK cells in which synthesis of laminin α3 is suppressed is severely inhibited (Figure 8). Others previously observed that function-blocking antibodies against laminin α3 inhibited proliferation of both the rat bladder carcinoma cell line 804G and the human mammary carcinoma cell line MCF-10A (Gonzales *et al*., 1999). The proliferation signal was believed to be transduced from the laminin α3 G domain through integrin α3β1, and seemed to involve ERK signaling. A proliferation defect was also found in mouse keratinocytes expressing deleted β4 integrin when plated on LN5, suggesting, in this case, that the proliferation signal was transduced by α6β4 integrin instead of α3β1 (Nikolopoulos *et al*., 2005). Although our results with MDCK cells generally agree with these findings, we have not yet determined which integrin receptors or signaling intermediates are involved in proliferation.

LN5 and Apical–Basal Polarization

When MDCK cells in which laminin α3 synthesis was suppressed were plated at high density on permeable supports, they were able to polarize, even though the epithelium formed was abnormal in morphology (Figure 10). This result, along with our other observations, would seem to suggest that LN5 is important for reestablishing the continuity of an incomplete epithelium, but not for determining orientation of the apical-basal axis once epithelial integrity is restored. This conclusion would seem to be reinforced by recent experiments suggesting that assembly of laminin into a basal lamina is critical for polarization of MDCK cells grown in three-dimensional collagen I gels. Because biochemical studies indicate that LN5 is incapable of self-assembly (Cheng *et al*., 1997), it is more likely that another laminin isoform, such as LN10, is responsible for polarization. LN10 is structurally similar to LN1, which can self-assemble and is required for polarization of mouse embryonic stem cell epiblasts (Li *et al*., 2003; Miner and Yurchenco, 2004).

On the other hand, it may be premature to conclude that LN5 plays no role in the overall process of polarization. LN5 is unable to either self-assemble or copolymerize with other, full-length laminin isoforms in solution (Cheng *et al*., 1997). However, recent biochemical studies with recombinant laminin amino-terminal globular domains have demonstrated interactions between both a recombinant laminin β3 fragment and complete keratinocyte LN5 and laminin γ1, a component of both LN1 and LN10, by surface plasmon resonance (Odenthal *et al*., 2004). On this basis, it may be reasonable to postulate that the provisional LN5 matrix deposited during epithelial regeneration serves as a template for a more rigid and permanent LN10 basal lamina.

If true, then why would knockdown of LN5 not block polarization of MDCK cells? Our polarization experiments were conducted on Transwell permeable supports (Figure 10). Despite the presence of pores, areas of the support between the pores might form a permeability barrier that traps and concentrates secreted LN10 beneath the cell. Under these conditions, assembly of LN10 into a basal lamina might occur spontaneously without the need for a LN5 provisional matrix. In contrast, such a permeability barrier would not exist in three-dimensional collagen gels, where the requirement for basal lamina assembly for polarization has been demonstrated. The observation that both function-blocking antibodies against β1 integrin and expression of dominant-negative Rac1 block laminin assembly and MDCK cell polarization in three-dimensional collagen gels but not in two-dimensional cultures is consistent with this interpretation (O'Brien *et al*., 2001; Yu *et al*., 2005). Future experiments in our laboratory designed to look more directly at the relationships between LN5 expression and assembly of LN10 into a basal lamina are designed to test these ideas.

ACKNOWLEDGMENTS

We are grateful to Mirjam Zegers and Martin ter Beest (University of Cincinnati) for helpful suggestions and critical review of the manuscript, to Nancy Kleene and the Advanced Microscopy Core Facility at the University of Cincinnati for help with confocal microscopy and MetaMorph, to Aki Manninen (Max Planck Institute for Molecular Cell Biology and Genetics, Dresden, Germany) for assistance with adenovirus production, and to Monique Aumailley (University of Cologne, Cologne, Germany) for stimulating discussions and providing unpublished results. Financial support was provided by National Institutes of Health (NIH) Grant T32 DK-64581, a Shriners Hospital for Children Fellowship, and an Ethicon-Society of University Surgeons Surgical Research Fellowship (to G.Z.M.); by American Cancer Society Research Scholar Grant RSG-04–251-01-CCG (to K.H.G.); and by NIH Grant R01 DK-046768 and the Department of Surgery, University of Cincinnati (to K.S.M.). M.K. was supported by Grant SFB 589 from the Deutsche Forschungsgemeinschaft.

REFERENCES

Aumailley, M., El Khal, A., Knoss, N., and Tunggal, L. (2003). Laminin 5 processing and its integration into the ECM. Matrix Biol. *22*, 49–54.

Boll, W., Partin, J. S., Katz, A. I., Caplan, M. J., and Jamieson, J. D. (1991). Distinct pathways for basolateral targeting of membrane and secretory proteins in polarized epithelial cells. Proc. Natl. Acad. Sci. USA *88*, 8592–8596.

Caplan, M. J., Stow, J. L., Newman, A. P., Madri, J., Anderson, H. C., Farquhar, M. G., Palade, G. E., and Jamieson, J. D. (1987). Dependence on pH of polarized sorting of secreted proteins. Nature *329*, 632–635.

Carter, W. G., Ryan, M. C., and Gahr, P. J. (1991). Epiligrin, a new cell adhesion ligand for integrin $\alpha 3\beta 1$ in epithelial basement membranes. Cell *65*, 599–610.

Cheng, Y. S., Champliaud, M. F., Burgeson, R. E., Marinkovich, M. P., and Yurchenco, P. D. (1997). Self-assembly of laminin isoforms. J. Biol. Chem. *272*, 31525–31532.

Colognato, H., Winkelmann, D. A., and Yurchenco, P. D. (1999). Laminin polymerization induces a receptor-cytoskeleton network. J. Cell Biol. *145*, 619–631.

Colognato, H., and Yurchenco, P. D. (2000). Form and function: the laminin family of heterotrimers. Dev. Dyn. *218*, 213–234.

Decline, F., and Rousselle, P. (2000). Keratinocyte migration requires $\alpha 2\beta 1$ integrin-mediated interaction with the laminin 5 $\gamma 2$ chain. J. Cell Sc. *114*, 811–823.

Eble, J. A., Wucherpfennig, K. W., Gauthier, L., Dersch, P., Krukonis, E., Isberg, R. R., and Hemler, M. E. (1998). Recombinant soluble human alpha 3 beta 1 integrin: purification, processing, regulation, and specific binding to laminin-5 and invasin in a mutually exclusive manner. Biochemistry *37*, 10945–10955.

Ekblom, P., Forsberg, E., Gullberg, D., and Ekblom, M. (1999). Laminin isoforms and epithelial development. In: Epithelial Morphogenesis in Development and Disease, ed. W. Birchmeier and C. Birchmeier, Amsterdam: Harwood Academic Publishers, 261–286.

Elbashir, S. M., Harborth, J., Lendeckel, W., Yalcin, A., Weber, K., and Tuschl, T. (2001). Duplexes of 21-nucleotide RNAs mediate RNA interference in cultured mammalian cells. Nature *411*, 494–498.

Elbashir, S. M., Harborth, J., Weber, K., and Tuschl, T. (2002). Analysis of gene function in somatic mammalian cells using small interfering RNAs. Methods *26*, 199–213.

Fish, E. M., and Molitoris, B. A. (1994). Alterations in epithelial polarity and the pathogenesis of disease. N. Engl. J. Med. 1580–1588.

Frank, D. E., and Carter, W. G. (2004). Laminin 5 deposition regulates keratinocyte polarization and persistent migration. J. Cell Sci. *117*, 1351–1363.

Ghosh, S., and Stack, M. S. (2000). Proteolytic modification of laminins: functional consequences. Microsc. Res. Tech. *51*, 238–246.

Giannelli, G., and Antonaci, S. (2000). Biological and clinical relevance of laminin-5 in cancer. Clin. Exp. Metastasis *18*, 439–443.

Giannelli, G., Falk-Marzillier, J., Schiraldi, O., Stetler-Stevenson, W. G., and Quaranta, V. (1997). Induction of cell migration by matrix metalloprotease-2 cleavage of laminin-5. Science *277*, 225–228.

Goldfinger, L. E., Stack, M. S., and Jones, J. C. (1998). Processing of laminin-5 and its functional consequences: role of plasmin and tissue-type plasminogen activator. J. Cell Biol. *141*, 255–265.

Gonzales, M., Haan, K., Baker, S. E., Fitchmun, M., Todorov, I., Weitzman, S., and Jones, J. C. (1999). A cell signal pathway involving laminin-5, alpha3beta1 integrin, and mitogen-activated protein kinase can regulate epithelial cell proliferation. Mol. Biol. Cell *10*, 259–270.

Gumbiner, B., and Simons, K. (1986). A functional assay for proteins involved in establishing an epithelial occluding barrier: identification of a uvomorulin-like polypeptide. J. Cell Biol. *102*, 457–468.

Hall, D. E., Reichardt, L. F., Crowley, E., Holley, B., Moezzi, H., Sonnenberg, A., and Damsky, C. H. (1990). The $\alpha 1/\beta 1$ and $\alpha 6/\beta 1$ integrin heterodimers mediate cell attachment to distinct sites on laminin. J. Cell Biol. *110*, 2175–2184.

Hintermann, E., and Quaranta, V. (2004). Epithelial cell motility on laminin-5, regulation by matrix assembly, proteolysis, integrins and erbB receptors. Matrix Biol. *23*, 75–85.

Hirosaki, T., Mizushima, H., Tsubota, Y., Moriyama, K., and Miyazaki, K. (2000). Structural requirement of carboxyl-terminal globular domains of laminin alpha 3 chain for promotion of rapid cell adhesion and migration by laminin-5. J. Biol. Chem. *275*, 22495–22502.

Jaffe, A. B., and Hall, A. (2005). Rho GTPases: biochemistry and biology. Annu. Rev. Cell Dev. Biol. *21*, 247–269.

Joly, D., Morel, V., Hummel, A., Ruello, A., Nusbaum, P., Patey, N., Noel, L. H., Rousselle, P., and Knebelmann, B. (2003). Beta4 integrin and laminin 5 are aberrantly expressed in polycystic kidney disease: role in increased cell adhesion and migration. Am. J. Pathol. *163*, 1791–1800.

Kariya, Y., Ishida, K., Tsubota, Y., Nakashima, Y., Hirosaki, T., Ogawa, T., and Miyazaki, K. (2002). Efficient expression system of human recombinant laminin-5. J. Biochem. *132*, 607–612.

Klein, G., Langegger, M., Timpl, R., and Ekblom, P. (1988). Role of the laminin A chain in the development of epithelial cell polarity. Cell *55*, 331–341.

Korang, K., Christiano, A. M., Uitto, J., and Mauviel, A. (1995). Differential cytokine modulation of the genes LAMA3, LAMB3, and LAMC2, encoding the constitutive polypeptides, alpha 3, beta 3, and gamma 2, of human laminin 5 in epidermal keratinocytes. FEBS Lett. *368*, 556–558.

Koshikawa, N., Giannelli, G., Cirulli, V., Miyazaki, K., and Quaranta, V. (2000). Role of cell surface metalloprotease MT1-MMP in epithelial cell migration over laminin-5. J. Cell Biol. *148*, 615–624.

Kreidberg, J. A. (2000). Functions of alpha3beta1 integrin. Curr. Opin. Cell Biol. *12*, 548–553.

Kreidberg, J. A., and Symons, J. M. (2000). Integrins in kidney development, function, and disease. Am. J. Physiol. *279*, F233–F242.

Laemmli, U. K. (1970). Cleavage of structural proteins during the assembly of the head of bacteriophage T4. Nature *227*, 680–685.

Le Beyec, J., Delers, F., Jourdant, F., Schreider, C., Chambaz, J., Cardot, P., and Pincon-Raymond, M. (1997). A complete epithelial organization of Caco-2 cells induces I-FABP and potentializes apolipoprotein gene expression. Exp. Cell Res. *236*, 311–320.

Li, S., Edgar, D., Fassler, R., Wadsworth, W., and Yurchenco, P. D. (2003). The role of laminin in embryonic cell polarization and tissue organization. Dev. Cell *4*, 613–624.

Li, S., Liquari, P., McKee, K. K., Harrison, D., Patel, R., Lee, S., and Yurchenco, P. D. (2005). Laminin-sulfatide binding initiates basement membrane assembly and enables receptor signaling in Schwann cells and fibroblasts. J. Cell Biol. *169*, 179–189.

Marinkovich, M. P., Lunstrum, G. P., and Burgeson, R. E. (1992). The anchoring filament protein kalinin is synthesized and secreted as a high molecular weight precursor. J. Biol. Chem. *267*, 17900–17906.

Matlin, K. S., Reggio, H., Helenius, A., and Simons, K. (1981). Infectious entry pathway of influenza virus in a canine kidney cell line. J. Cell Biol. *91*, 601–613.

Meder, D., Shevchenko, A., Simons, K., and Fullekrug, J. (2005). Gp135/podocalyxin and NHERF-2 participate in the formation of a preapical domain during polarization of MDCK cells. J. Cell Biol. *168*, 303–313.

Miller, K. A., Chung, J., Lo, D., Jones, J. C., Thimmapaya, B., and Weitzman, S. A. (2000). Inhibition of laminin-5 production in breast epithelial cells by overexpression of p300. J. Biol. Chem. *275*, 8176–8182.

Miner, J. H. (1999). Renal basement membrane components. Kidney Int. *56*, 2016–2024.

Miner, J. H., and Yurchenco, P. D. (2004). Laminin Functions in Tissue Morphogenesis. Annu. Rev. Cell Dev. Biol. *20*, 255–284.

Miyazaki, K., Kikkawa, Y., Nakamura, A., Yasumitsu, H., and Umeda, M. (1993). A large cell-adhesive scatter factor secreted by human gastric carcinoma cells. Proc. Natl. Acad. Sci. USA *90*, 11767–11771.

Nelson, W. J. (2003). Adaptation of core mechanisms to generate cell polarity. Nature *422*, 766–774.

Nguyen, B. P., Gil, S. G., and Carter, W. G. (2000a). Deposition of laminin 5 by keratinocytes regulates integrin adhesion and signaling. J. Biol. Chem. *275*, 31896–31907.

Nguyen, B. P., Ren, X. D., Schwartz, M. A., and Carter, W. G. (2001). Ligation of integrin alpha 3beta 1 by laminin 5 at the wound edge activates Rho-dependent adhesion of leading keratinocytes on collagen. J. Biol. Chem. *276*, 43860–43870.

Nguyen, B. P., Ryan, M. C., Gil, S. G., and Carter, W. G. (2000b). Deposition of laminin 5 in epidermal wounds regulates integrin signaling and adhesion. Curr. Opin. Cell Biol. *12*, 554–562.

Niessen, C. M., Hogervorst, F., Jaspars, L. H., de Melker, A. A., Delwel, G. O., Hulsman, E.H.M., Kuikman, I., and Sonnenberg, A. (1994). The $\alpha 6\beta 4$ integrin is a receptor for both laminin and kalinin. Exp. Cell Res. *211*. 360–367.

Nikolopoulos, S. N., Blaikie, P., Yoshioka, T., Guo, W., Puri, C., Tacchetti, C., and Giancotti, F. G. (2005). Targeted deletion of the integrin beta4 signaling

domain suppresses laminin-5-dependent nuclear entry of mitogen-activated protein kinases and NF-kappaB, causing defects in epidermal growth and migration. Mol. Cell. Biol. *25*, 6090–6102.

O'Brien, L. E., Jou, T. S., Pollack, A. L., Zhang, Q., Hansen, S. H., Yurchenco, P., and Mostov, K. E. (2001). Rac1 orientates epithelial apical polarity through effects on basolateral laminin assembly. Nat. Cell Biol. *3*, 831–838.

Odenthal, U., Haehn, S., Tunggal, P., Merkl, B., Schomburg, D., Frie, C., Paulsson, M., and Smyth, N. (2004). Molecular analysis of laminin N-terminal domains mediating self-interactions. J. Biol. Chem. *279*, 44504–44512.

Ojakian, G. K., and Schwimmer, R. (1988). The polarized distribution of an apical cell surface glycoprotein is maintained by interactions with the cytoskeleton of Madin-Darby canine kidney cells. J. Cell Biol. *107*, 2377–2387.

O'Toole, E. A., Marinkovich, M. P., Hoeffler, W. K., Furthmayr, H., and Woodley, D. T. (1997). Laminin-5 inhibits human keratinocyte migration. Exp. Cell Res. *233*, 330–339.

Prahalad, P., Calvo, I., Waechter, H., Matthews, J. B., Zuk, A., and Matlin, K. S. (2004). Regulation of MDCK cell-substratum adhesion by RhoA and myosin light chain kinase after ATP depletion. Am. J. Physiol. *286*, C693–C707.

Rousselle, P., Lunstrum, G. P., Keene, D. R., and Burgeson, R. E. (1991). Kalinin: an epithelium-specific basement membrane adhesion molecule that is a component of anchoring filaments. J. Cell Biol. *114*, 567–576.

Schoenenberger, C.-A., Zuk, A., Zinkl, G. M., Kendall, D., and Matlin, K. S. (1994). Integrin expression and localization in normal MDCK cells and transformed MDCK cells lacking apical polarity. J. Cell Sci. *107*, 527–541.

Sonnenberg, A., Janssen, H., Hogervorst, F., Calafat, J., and Hilgers, J. (1987). A complex of platelet glycoproteins Ic and IIa identified by a rat mAb. J. Biol. Chem. *262*, 10376–10383.

Sorokin, L. A., Sonnenberg, A., Aumailley, M., Timpl, R., and Ekblom, P. (1990). Recognition of the laminin E8 cell-binding site by an integrin possessing the α6 subunit is essential for epithelial polarization in developing kidney tubules. J. Cell Biol. *111*, 1265–1274.

Vega-Salas, D. E., Salas, P.J.I., Gundersen, D., and Rodriguez-Boulan, E. (1987). Formation of the apical pole of epithelial (Madin-Darby kidney) cells: polarity of an apical protein is independent of tight junctions while segregation of a basolateral marker requires cell-cell interactions. J. Cell Biol. *104*, 905–916.

Yu, W., Datta, A., Leroy, P., O'Brien, L. E., Mak, G., Jou, T. S., Matlin, K. S., Mostov, K. E., and Zegers, M. M. (2005). Beta1-integrin orients epithelial polarity via Rac1 and laminin. Mol. Biol. Cell *16*, 433–445.

Yurchenco, P. D. (1994). Assembly of laminin and type IV collagen into basement membrane networks. In: Extracellular Matrix Assembly and Structure, ed. P. D. Yurchenco, D. E. Birk, and R. P. Mecham, San Diego: Academic Press, 351–388.

Zhang, K., and Kramer, R. H. (1996). Laminin 5 deposition promotes keratinocyte motility. Exp. Cell Res. *227*, 309–322.

Zinkl, G. M., Zuk, A., van der Bijl, P., van Meer, G., and Matlin, K. S. (1996). An antiglycolipid antibody inhibits Madin-Darby canine kidney cell adhesion to laminin and interferes with basolateral polarization and tight junction formation. J. Cell Biol. *133*, 695–708.

Zuk, A., Bonventre, J. V., Brown, D., and Matlin, K. S. (1998). Polarity, integrin, and extracellular matrix dynamics in the postischemic rat kidney. Am. J. Physiol. *275*, C711–C731.

Zuk, A., and Matlin, K. S. (2002). Induction of a laminin isoform and the $\alpha 3\beta 1$ integrin in renal ischemic injury and repair in vivo. Am. J. Physiol. *283*, F971–F984.